Atmospheric Research 326 (2025) 108312

Contents lists available at ScienceDirect

Atmospheric Research

journal homepage: www.elsevier.com/locate/atmosres

Comprehensive Lagrangian assessment of Canary Island precipitation moisture sources

Gleisis Alvarez-Socorro [a,*], José Carlos Fernández-Alvarez [a,b,c], Luis Cana [d], David Suárez-Molina [e], Raquel Nieto [a,b], Luis Gimeno [a,b]

[a] Centro de Investigación Mariña, Universidade de Vigo, Environmental Physics Laboratory (EPhysLab), Campus As Lagoas s/n, 32004 Ourense, Spain
[b] Galicia Supercomputing Center (CESGA), Avenida de Vigo, 3, 15705 Santiago de Compostela, Spain
[c] CESAM, Departamento de Física, Universidade de Aveiro, 3810-193 Aveiro, Portugal
[d] Unidad de Océano y Clima, Instituto de Oceanografía y Cambio Global, IOCAG, Universidad de Las Palmas de Gran Canaria, 35017 Las Palmas de Gran Canaria, Spain
[e] Delegation of AEMET in the Canary Islands (DTCAN), State Meteorological Agency of Spain (AEMET), 35017 Las Palmas de Gran Canaria, Spain

ARTICLE INFO

Keywords:
Moisture source
Dynamical downscaling
Lagrangian methodology
FLEXPART-WRF
Canary Islands
Trade wind inversion layer

ABSTRACT

The Canary Archipelago, due to its location between the tropics and subtropics, represents a key region for studying precipitation moisture sources. This study provides a high-resolution (20 km) climatological analysis of the moisture sources for potential precipitation in the archipelago from 1985 to 2022, applying a dynamic downscaling methodology (WRF-ARW) and a Lagrangian approach considering the trajectories of potentially precipitating particles (FLEXPART-WRF model). The analysis differentiates between precipitation and non-precipitation days, western and eastern islands, and moisture transport above and below the trade wind inversion layer (at 900 hPa). Results indicate that the main moisture source for the archipelago is the North Atlantic (up to 74 % annually), and a crucial contribution comes from the northeast region of the islands, especially under prevailing trade wind conditions. During the summer, moisture from the African continent further enhances its contribution up to 16 % for the total moisture transported. The moisture pattern is more pronounced on days with precipitation, extending longitudinally towards the western Atlantic, and showing the largest positive anomalies during intense precipitation events. Notably, our findings highlight the strong contribution of moisture from the northeast above the inversion layer, even on non-precipitation days. Additionally, differences in precipitation moisture source patterns were observed between the eastern and western islands, with positive anomalies in the northern sector for the former and the western one for the latter, each associated with different circulation patterns.

1. Introduction

The Canary Islands, part of Spain, are located near the north-western coast of the Sahara, between latitudes 29.5° N and 27.5° N and longitudes 18° W and 13.5° W. The archipelago covers an area of around 7447 km^2 and comprises seven volcanic islands and several islets, forming the provinces of Las Palmas and Santa Cruz de Tenerife (Francisco-Ortega et al., 2009). These islands exhibit a peculiar climate that is influenced by a range of environmental factors, including the predominant north-east trade winds, the semi-permanent Azores High-pressure system, and the strong influence of the cold oceanic current of the Canary Islands. They are also influenced by the surrounding ocean, altitude, occasional dry winds from the Sahara, and their diverse topography (Cropper and Hanna, 2014).

Precipitation in the Canary Islands is mainly controlled by altitude and the orientation of the dominant wind direction. The trade winds transport moist air masses, which lead to orographic condensation and subsequent precipitation as they rise over the island slopes (Herrera et al., 2001). This results in higher precipitation in the northern and northeastern parts of the higher islands. In contrast, Lanzarote and Fuerteventura receive minimal precipitation due to their lower elevation and proximity to the African continent, corresponding to their arid climate. While the northern parts of the high islands receive around 1000 mm of rainfall per year, the southern parts of these islands and the

* Corresponding author.
E-mail address: gleisis.alvarez.socorro@uvigo.es (G. Alvarez-Socorro).

https://doi.org/10.1016/j.atmosres.2025.108312
Received 25 March 2025; Received in revised form 20 June 2025; Accepted 20 June 2025
Available online 21 June 2025

flatter islands receive an average rainfall of around 200 mm per year (AEMET, 2012; Pérez et al., 2014). According to Bechtel (2016), the analysis of annual cycle parameters, which provide a global climatology of the annual land surface temperature, clearly showed the differences between the flatter and higher islands, as well as between the northern and southern slopes of the Canary Islands archipelago. Additionally, Ramos et al. (2018) noted that the influence of atmospheric rivers on extreme precipitation events in the Canary Islands is relatively low, accounting for less than 50 %. The atmospheric rivers predominantly affect the western islands, with the highest precipitation values observed at the highest altitude areas, while islands such as La Palma and Lanzarote experience less than 30 % influence from atmospheric rivers.

Moisture sources play a key role in atmospheric dynamics, especially in island regions such as the Canary Islands archipelago. Due to their geographical location, these islands are located in a transitional climate zone between temperate and tropical regions, making them susceptible to different atmospheric influences. They are therefore influenced by the variety of factors commented above as well as by modes of climatic variability such as the North Atlantic Oscillation (Herrera et al., 2001). These elements interact in complex ways, contributing to the unique climatic characteristics of the Canary Islands. Therefore, it is essential to study the behaviour of different moisture sources and their influence on the climate of this region and on the formation of relevant meteorological events, such as precipitation. In this region, monthly rainfall exhibits pronounced seasonality, with December and January being the wettest months, while July and August record the driest months (AEMET, 2012). In addition, the tropical latitude of the Canary Islands makes them more prone to convective rainfall, even in winter (García-Herrera et al., 2003).

Several studies have focused on analysing of the air masses using isentropic back-trajectories (Sancho et al., 1992; Viana et al., 2002; Rodríguez et al., 2004; Guerra et al., 2004; Izquierdo et al., 2011), finding that air masses reaching the Canary Islands archipelago come directly from the North Atlantic throughout the year. This suggests that the North Atlantic is the main moisture source for the region (Guerra et al., 2023). During winter, additional contributions arise from other regions, with air masses travelling from Europe, either via the Mediterranean Sea (Bershaw, 2018) or, even, by crossing North Africa (Dahinden et al., 2021). Furthermore, Herrera et al. (2001) found that low to moderate rainfall totals ($P < 100$ mm) are associated with a wide range of moisture sources, including the North Atlantic, Mediterranean, and local sources, etc. These sources combined with several synoptic climatic conditions, which are likely to produce rainfall with a wide range of isotopic compositions from very different processes.

Numerical models can be categorized as either Eulerian or Lagrangian, depending on how they formulate the transport problem, as reviewed by Gimeno et al. (2020). Eulerian models compute the concentrations and fluxes of traced moisture within a control volume (e.g., Arnault et al., 2021; Dahinden et al., 2023; Insua-Costa and Miguez-Macho, 2018; Van der Ent et al., 2014). Several studies have applied this approach to investigate the sources of moisture that contribute to precipitation in various regions, for instance using the Water Accounting Model-2-layers (Zhou and Shi, 2024; Zhao et al., 2024; Li et al., 2024). While, Lagrangian models track individual air parcels as they are transported by the ambient flow (e.g., Cheng and Lu, 2023; Keune et al., 2022; Holgate et al., 2020; Tuinenburg and Staal, 2020; Sodemann et al., 2008).

According to previous studies, no analysis of the moisture sources affecting the Canary Islands has yet been carried out using a Lagrangian approach. This approach to moisture tracking provides high-resolution diagnostics of moisture sources and enables a quantitative assessment of their origin. This method offers realistic air parcel trajectories, is computationally efficient, and complements Eulerian methods by providing a more comprehensive understanding of atmospheric moisture transport. In addition, the marked differences in precipitation across the archipelago, mentioned above, suggest variations in the moisture sources associated with their sinks. By expanding the analysis under different conditions —comparing the behaviour of moisture sources on days with and without precipitation, as well as their most extreme quantiles, the differences between the western and eastern islands, and considering the layers above and below 900 hPa— valuable insights can be gained from both scientific and practical perspectives. Therefore, the main objective of this study is to analyse the behaviour of moisture sources affecting the Canary Archipelago, using high-resolution atmospheric models, such as WRF-ARW and FLEXPART-WRF, within a Lagrangian framework. Given its geographical position, this region is particularly strategic for this type of analysis, as it can be highly affected by the unequal behaviour of the humidity input under different atmospheric conditions.

2. Methods and data

2.1. Data used

2.1.1. ERA5 Reanalysis data

ERA5 reanalysis data (Hersbach et al., 2020) was used as initial and boundary conditions to force the Weather Research and Forecasting model (WRFv3.8.1) with its dynamic ARW core (WRF-ARW) (Skamarock et al., 2008). ERA5 represents the latest and most advanced (fifth generation) reanalysis product from the European Centre for Medium-Range Weather Forecasts (ECMWF). It features a spatial resolution of 31 km and a temporal resolution of 1 h, offering a detailed representation of variables across 137 vertical levels. In particular, the number of assimilated observations has increased to about 24 million per day in 2019. Specifically, 94.6 billion observations have been actively assimilated in four dimensions (4D-Var), 65 million in the ocean wave component and 1 billion corresponding to surface air temperature and relative humidity (Hersbach et al., 2020). In addition, ERA5 provides a better representation of precipitation fields over different oceanic regions, both tropical and extratropical, due to significant improvements in warm rain and ice-phase processes, ice oversaturation and improved representation of mixed-phase clouds, as well as rain and snow precipitation forecast variables.

2.1.2. Precipitation data

The precipitation data were obtained from AEMET's National Climate Data Bank. These data have been recorded by AEMET's in-situ observation network across the Canary Islands. This study considers 24-h accumulated precipitation values, including only records exceeding a threshold of 1 mm per day (Polade et al., 2014; Schär et al., 2016) for subsequent analyses.

2.2. WRF and FLEXPART-WRF model configurations used in dynamic downscaling

To obtain a better resolution and improve the physical characterisation of our results, a dynamic downscaling of ERA5 data at 0.25 degrees was performed using the WRF-ARW model (version 3.8.1; Skamarock et al., 2008). The mesh used is composed of 480 × 800 horizontal latitude/longitude grids and 40 vertical sigma levels extending from the surface to 50 hPa. It covers the area of 115.39°W to 42.02°W and 19.41°S to 59.51°N (Fig. 1, red outline), achieving a spatial resolution of ≈20 km (0.18 degrees). The selection of physical configurations used here was based on those proposed and validated in previous studies (e.g., Insua-Costa and Miguez-Macho, 2018; Insua-Costa et al., 2019; Fernández-Alvarez et al., 2023b; Fernández-Alvarez et al., 2023c). For more details on the model configuration see Tables S1 and S2 in the Supplementary Material. For the dynamic downscaling, a set of key atmospheric variables has been selected to represent both the vertical structure of the atmosphere and surface conditions. At vertical levels, the variables include geopotential, relative humidity, temperature, and the zonal and meridional wind components. At the surface, the

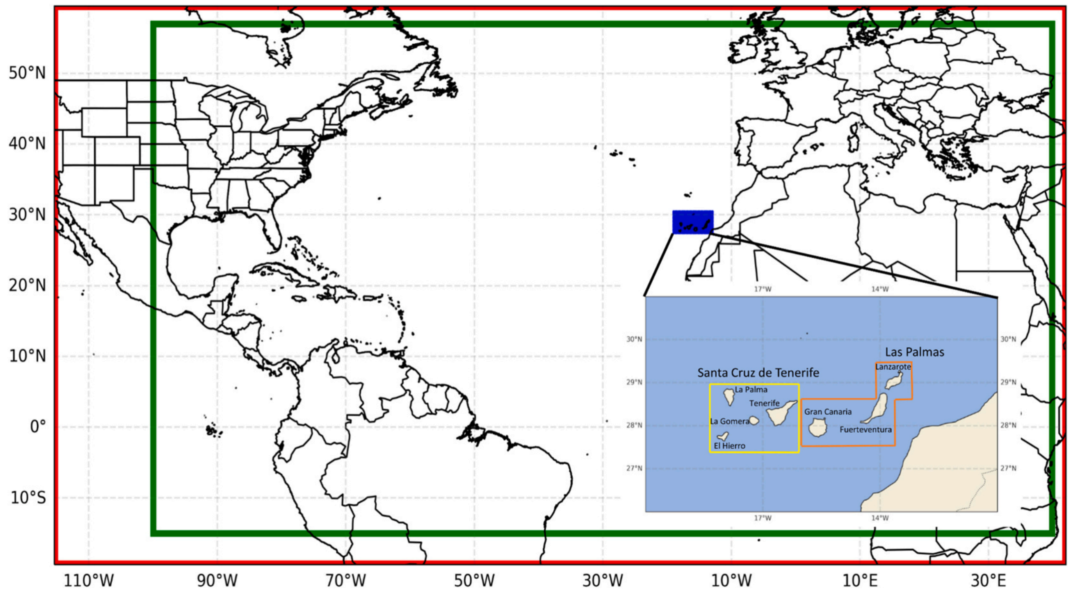

Fig. 1. Simulation domains for WRF-ERA5 (red) [115.39°W to 42.02°E and 19.41°S to 59.51°N] and FLEXPART-WRF (green) [100 to 40°W and 15°S to 57°N]. The target study region, the Canary Islands archipelago, is marked in blue. The geographical region for eastern and western islands of the archipelago, is marked in orange and yellow, respectively. (For interpretation of the references to colour in this figure legend, the reader is referred to the web version of this article.)

dataset comprises 10-m wind, 2-m temperature and dew point temperature, surface pressure, mean sea level pressure, land-sea mask, snowfall-related variables (including snowfall rate, snow depth, and snow density), surface geopotential, sea ice cover, sea surface temperature, skin temperature, soil temperature at four depths, and volumetric soil moisture at four layers. Together, these variables provide the necessary boundary and initial conditions to accurately force regional climate models and capture essential physical processes in high-resolution simulations.

The WRF-ARW model outputs forced with the ERA5 data (hereafter WRF-ERA5) were used as initial and boundary conditions for the regional particle dispersion model FLEXible PARTicle (FLEXPART-WRF) version 3.3.2 (Brioude et al., 2013). The FLEXPART-WRF outputs, with a resolution of 0.18 degrees in a 400 × 777 grid, cover the area of 100°W to 40°E and 15°S to 57°N (Fig. 1, green box), were used to represent atmospheric transport to determine the sources of moisture for the Canary archipelago environment. During the lagrangian dispersion modelization, the mass balance for each particle is conveniently resolved in a 6-h time step for a total of 2 million particles. This number of particles ensures that at least one particle was assigned to each model grid point, thereby maintaining mass conservation. In addition, WRF-ARW and FLEXPART-WRF simulations were run annually, each preceded by a one-month spin-up to ensure proper initialization. WRF-ARW was executed first, and then FLEXPART-WRF. While WRF-ARW used a 60-s time step and required restart options in case of interruption, FLEXPART-WRF, being simpler and faster, also included restart functionality and consumed fewer computational resources.

This configuration, based on WRF-ARW coupled with FLEXPART-WRF, has been extensively evaluated in recent studies focused on high-resolution moisture transport across the North Atlantic Ocean (Fernández-Alvarez, 2023,Fernández-Alvarez et al., 2023b; 2025). Validation against global FLEXPART and ERA5 reanalysis over a 30-year period supports its suitability for Lagrangian analyses (Fernández-Alvarez, 2023). Although some biases exist —such as precipitation overestimation in tropical regions— WRF-ERA5 performs better in areas with complex topography and reproduces key features of the moisture budget. Its high spatial resolution (20 km) allows for a more detailed representation of local processes, making it particularly useful for identifying moisture sources and transport mechanisms.

The analysis covers the period from 1985 to 2022, considering the seasons as: January–March (JFM), April–June (AMJ), July–September (JAS), October–December (OND), as well the full annual period (ANNUAL).

2.3. Determination of moisture sources

The Lagrangian method proposed by Fremme and Sodemann (2019), which evaluates the Lagrangian water balance along the trajectories, was used to calculate the sources of moisture that potentially bring precipitation over the Canary Islands. This method allows the evolution of each particle, into which the atmosphere is divided, in terms of specific humidity (q) over time (t). The variations in q were analyzed in a 6-h temporal resolution. In an air parcel transported within the atmospheric flow, specific moisture is conserved unless evaporation or precipitation adds or removes moisture (Läderach and Sodemann, 2016), as expressed in the following equation:

$$(e-p) = m\left(\frac{dq}{dt}\right) \tag{1}$$

where m is the mass (considered constant) of the air parcel, d/dt is the derivative following the flow, q is the specific humidity, and (e-p) represents the increase or decrease in the water vapour ratio along the path (Stohl and James, 2004) measures in units of kg/s. Particles that are considered potentially precipitating are defined as those with a decrease in specific humidity of more than 0.1 g/kg in the 6 h before reaching the target region, as in Läderach and Sodemann (2016), which does not imply that precipitation occurs. The (e-p) values for each grid point were aggregated to calculate the moisture source pattern of these potentially precipitating particles. The particles were tracked for an initial period of ten days, the time considered as the residence time of water vapour in the atmosphere (Numaguti, 1999; Van Der Ent and Tuinenburg, 2017; Gimeno et al., 2021). Despite this, the limitations of using the Lagrangian approach must be considered. These include the possible overestimation of evaporation and precipitation values, since the approach does not distinguish both processes. Other limitations include the failure to take into account ice and liquid water, possible variations associated with non-physical processes determined by phenomenology, and the sensitivity of moisture flux computations to increases in data noise for shorter time periods or smaller regions (Insua-Costa and

Miguez-Macho, 2018).

The trajectory simulations were processed using the TROVA software (Fernández-Alvarez et al., 2022) to calculate the moisture sources. TROVA was selected for its advanced functionalities and proven validation in the study region. It supports moisture source and sink analysis using outputs from FLEXPART and FLEXPART-WRF at multiple resolutions, and implements Lagrangian methodologies such as those of Stohl and James (2004) and Fremme and Sodemann (2019). Developed in Python and Fortran with parallel computing, it enables efficient processing and vertical-layer analysis. TROVA has been successfully validated in both climatological and event-based studies across the North Atlantic basin (Fernández-Alvarez, 2023; Coll-Hidalgo et al., 2025; Eiras-Barca et al., 2025).

To determine the moisture sources associated with the Canary Islands, several peculiarities were taken into account to identify possible differences under different conditions. Firstly, the general moisture sources were analyzed for the whole period studied. To find the differences in the moisture sources on days with and without precipitation, the recorded dataset by the AEMET stations was used. In addition, precipitation days were also separated for the minimum and maximum precipitation quantiles to analyse the moisture sources. Given the distinct differences in precipitation patterns between the eastern and western islands of the archipelago (corresponding with the two provinces), the set of days was also divided into three groups: the first included days with precipitation in both provinces, Las Palmas and Santa Cruz de Tenerife; the second, days with precipitation only in Las Palmas; and the third group encompasses days with precipitation only in Santa Cruz de Tenerife.

3. Results and discussion

A detailed study of the moisture sources affecting the Canary Islands was done for the entire atmospheric column, as well as for the layers below and above the thermal inversion around 900 hPa. Carrillo et al. (2016), using around 20,000 soundings at two stations in the Canary Islands between 1980 and 2013, demonstrated the existence of this inversion layer associated with the upper part of the marine boundary layer (MBL) and the trade wind inversion, where an abrupt change in the water vapour mixing ratio is observed. The 900 hPa level value represents the average value as its position varies seasonally and latitudinally. Its altitude decreases during the summer months (950 hPa), with a reinforcement of the inversion, and increases (825 hPa) in winter. Furthermore, Romero Campos et al. (2011) highlighted that during the day, the lowest and most humid layer tends to concentrate between 500 and 1000 m for most of the year, except for the months of June, July, and August, when it concentrates below 500 m, both day and night.

Fig. 2 shows the moisture source patterns associated with the Canary Islands during the annual and seasonally study periods, for the total column and the layers below and above the trade wind inversion layer bounded at 900 hPa. For the whole atmospheric column (Fig. 2, first column), the main annual moisture source regions are generally observed located near the north-northeast of the archipelago, extending out into the North Atlantic. This pattern is likely driven by the influence of the relatively humid northeast trade winds coming from the southern edge of the Azores anticyclone and the cold oceanic current that surrounds the archipelago (García de Pedraza, 1980; Martín et al., 2012; Mestre-Barceló et al., 2012). The North Atlantic provides the main

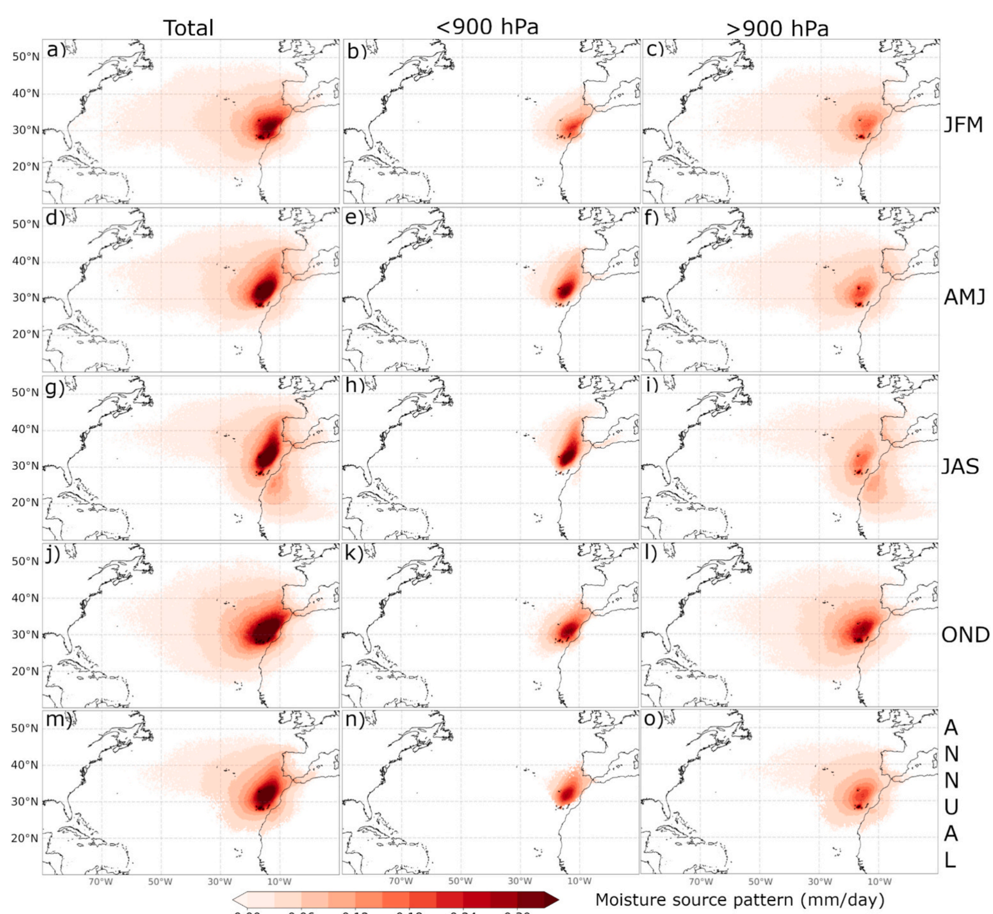

Fig. 2. Seasonal and annual moisture sources patterns (in mm/day) contributing to the Canary Islands from 1985 to 2022. From top to bottom, the seasonal periods: JFM (January–March), AMJ (April–June), JAS (July–September), and OND (October–December), and the annual mean. The columns, from left to right, show the moisture fields for the entire atmospheric vertical column, the layer from the surface to 900 hPa, and the layer above 900 hPa.

moisture for the islands, approximately the 74 % (ranging from 81 % in autumn to 63 % in summer) of the moisture, with respect to the total amount, followed by the African continent (9 % annually, reaching in summer up to 15,6 %) (Table S3 of the Supplementary Material).

Below 900 hPa (Fig. 2, central column) the moisture source field is more localized near the archipelago, especially in summer (JAS), with values exceeding 0.30 mm/day. This result supports the findings of Guerra et al. (2004), who proposed that the North Atlantic anticyclone strengthens the northeast trade winds, which blow with maximum frequency and intensity in summer in the cold and moist oceanic boundary layer below the inversion layer. The moisture contribution for the archipelago under this level oscillates across the year between 26 and 31 % (Table S4 of the Supplementary Material). Above 900 hPa (Fig. 2, third column) the spatial distribution of moisture sources in this layer closely resembles that of the whole column but with lower intensity, indicating a more diffuse and less direct transport of moisture at higher altitudes compared with the layer below 900 hPa. However, the percentage of moisture contribution in this layer is higher, with respect to the lowest one, between 69 and 74 % (maximum values in winter and minimum in spring, Table S4 Supplementary Material).

Specifically above 900 hPa, the North Atlantic region stands out, supporting approximately the 50 % of the humidity contribution in this layer all year round (Tabla S3 of the Supplementary Material). However, there are seasonal differences, especially in summer (JAS), when a northward shift of the moisture pattern occurs, and with an extra moisture intrusion from the African continent and even contributions from the Iberian Peninsula. During this period, the contribution from the North Atlantic decreased by up to 40 %, and it increased to 14.4 % from the African continent, and 2.8 % from southern Western Europe. This moisture from Africa above 900 hPa is associated with the presence of Sudano-Saharan disturbances and easterly waves near the archipelago. These easterly waves are more frequent in August and September, accounting for 64 %, of the total number of easterly waves affecting the Canary Islands (Sanz et al., 2022). In autumn, a slight southward shift in moisture sources is observed.

The observed changes in the moisture source patterns are linked to the shifts along the year of the Azores Anticyclone (Fig. 3, first column). The Azores Anticyclone is directly responsible for the weather in the Canary Islands. During winter it is usually located at low latitudes, between 30°N and 35°N. In summer, when it is further north, between 40°N and 45°N, the gradient weakens, allowing the northeast trade winds to blow and prevail, along with some warm disturbances associated with the Saharan thermal low (García de Pedraza, 1980). In the geopotential height fields (Fig. 3, second column), stable atmospheric conditions are observed, mainly during the spring and summer months; while in autumn and winter, a southward shift of positive geopotential height values is observed. Regarding integrated vertical moisture transport (IVT) (Fig. 3, last column), the dominant flux comes from the North Atlantic, adjacent to the Azores anticyclone, with greater intensity in spring and summer. Notably, in summer, unlike the rest of the

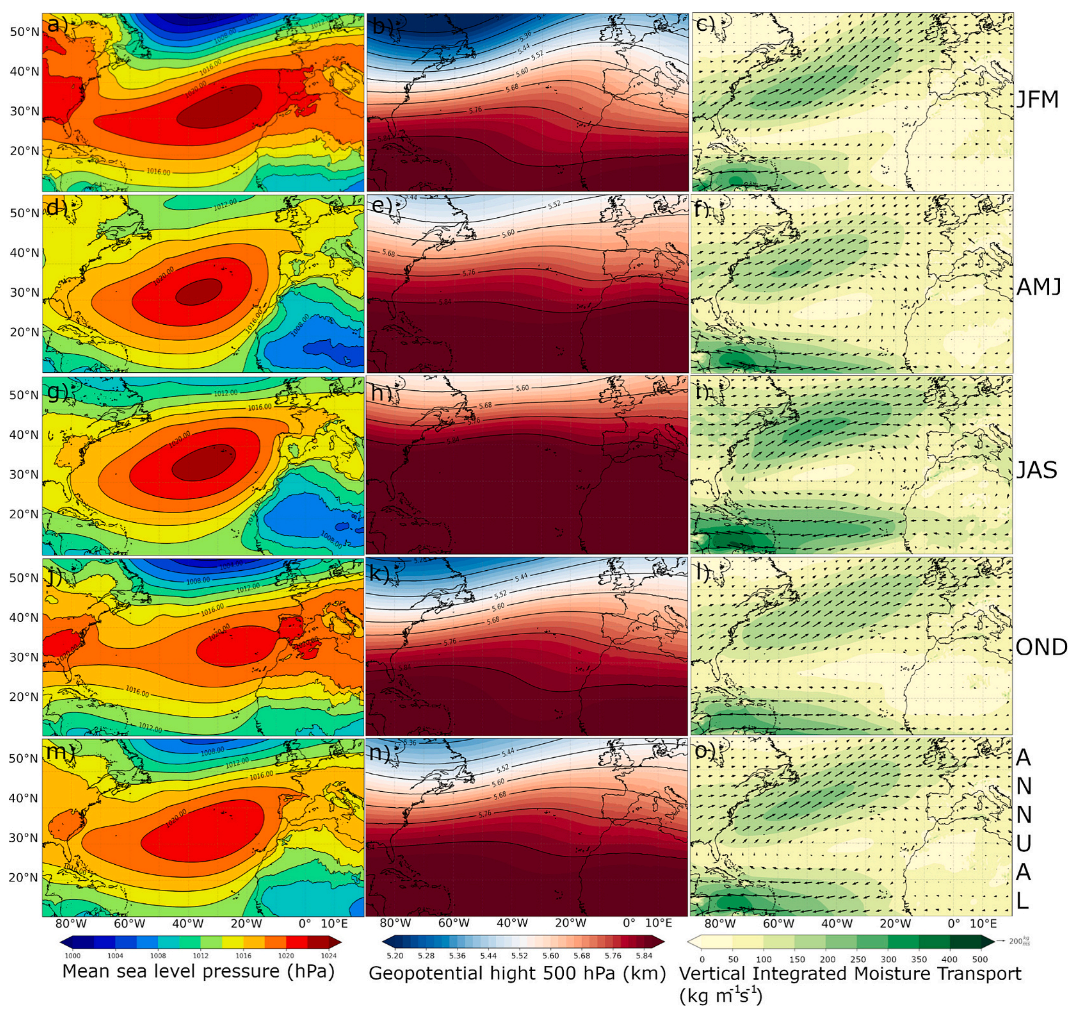

Fig. 3. Seasonal and annual patterns, from left to right columns, the mean sea level pressure (MSLP), geopotential height at 500 hPa, and vertically integrated moisture transport (IVT) for the period from 1985 to 2022 over the study area. Rows correspond to the seasonal periods: JFM (January–March), AMJ (April–June), JAS (July–September), OND (October–December), and the bottom row shows the annual average.

seasons, a flow from the African continent is observed, which corresponds to the primary moisture sources for this period. This flow is related to the disturbance of the Saharan outbreaks to the trade wind regime, during which the Saharan air layer is observed, generally above the MBL, mainly in summer (Rodríguez et al., 2011).

To better understand the differences in moisture source patterns above and below the 900 hPa level, we also analyzed the geopotential height fields at 950 hPa and 850 hPa, along with the IVT between 850 and 300 hPa, as shown in Fig. S2 of the Supplementary Material. Near the target region, in all cases, a well-defined center of high geopotential values is observed in the 850 hPa geopotential height field, related to the Azore's high pressure. In summer, this pattern shifts northward, and another center of high geopotential height is highlighted over the African continent, enabling a confluence of northeast and southeast flows near the islands. This flow, as mentioned above, determines that, especially during the summer months, there is a contribution of moisture not only from the North Atlantic but also from the west of the African continent and southern Western Europe. However, the 950 hPa geopotential height fields reflect the behaviour of moisture sources in the lowest layer, located north-northeast of the islands, largely due to the high geopotential values over the North Atlantic and low geopotential values over Africa. On the other hand, the IVT fields between 850 and 300 hPa (Fig. S2, third column of the Supplementary Material) also show differences, especially in summer, when transport from Africa is observed, influencing the behaviour of moisture sources for this period.

A monthly analysis is carried out to find deeper differences in moisture sources above and below the trade wind inversion layer (Fig. 4 and Fig. 5). The results confirmed that the lower layer contains the highest moisture concentrations, following the direction of the trade winds with the circulation of the eastern branch of the Azores Anticyclone. The location to the north-northeast of the islands of the moisture sources in these cases is conditioned by the location of the high values of geopotential height in the North Atlantic and lower values over the African continent, mentioned above. The lowest contributions were observed in February, March, April and December, while the largest in June, July, September and October. Above 900 hPa, the moisture source pattern is much more extensive in latitude and longitude, reaching as far as the Gulf of Mexico in February, March, and April. During transition months, a weakening of the overall moisture source pattern in North Atlantic is observed, but with a notable increase in contributions from Africa especially in June–September, and less from southwestern Western Europe (see Fig. S3 of the Supplementary Material). These observed differences are related to the presence of two well-defined centers of high geopotential values in July–September, both in the North Atlantic and in Africa, enabling the confluence of both flows over the target region, together with the behaviour of the IVT observed for these months (Fig. S2 of the Supplementary Material). These results may be related to differences in the relative humidity gradient in subtropical regions, with the highest values in the lower layer and lower in the upper layer, according to Grindinger (1992). Furthermore, the existence of this inversion layer can act as a physical barrier to rising air, limiting the vertical development of clouds and confining most of the moisture to the levels below it.

The analysis was further extended by grouping the days with and without precipitation in the archipelago, based on reports from AEMET stations, to assess potential differences in moisture sources. Fig. 6 illustrates the moisture source patterns for both conditions, considering the total atmospheric column, the two layers below and above 900 hPa, as well as their anomalies. Over the study period, a total of 4809 days with precipitation and 9070 days without precipitation were recorded for at least one of the considered stations (see Precipitation data section for details).

The pattern of moisture sources, both for precipitation days and non-precipitation days (Fig. 6, first and second column), shows that the most important source extends along the coast of Africa, from the Canary Archipelago to the Iberian Peninsula, both above and below the layer of 900 hPa. The contributions of moisture sources with respect to the total of both layers were 74 % and 26 % for days with precipitation and 71 %

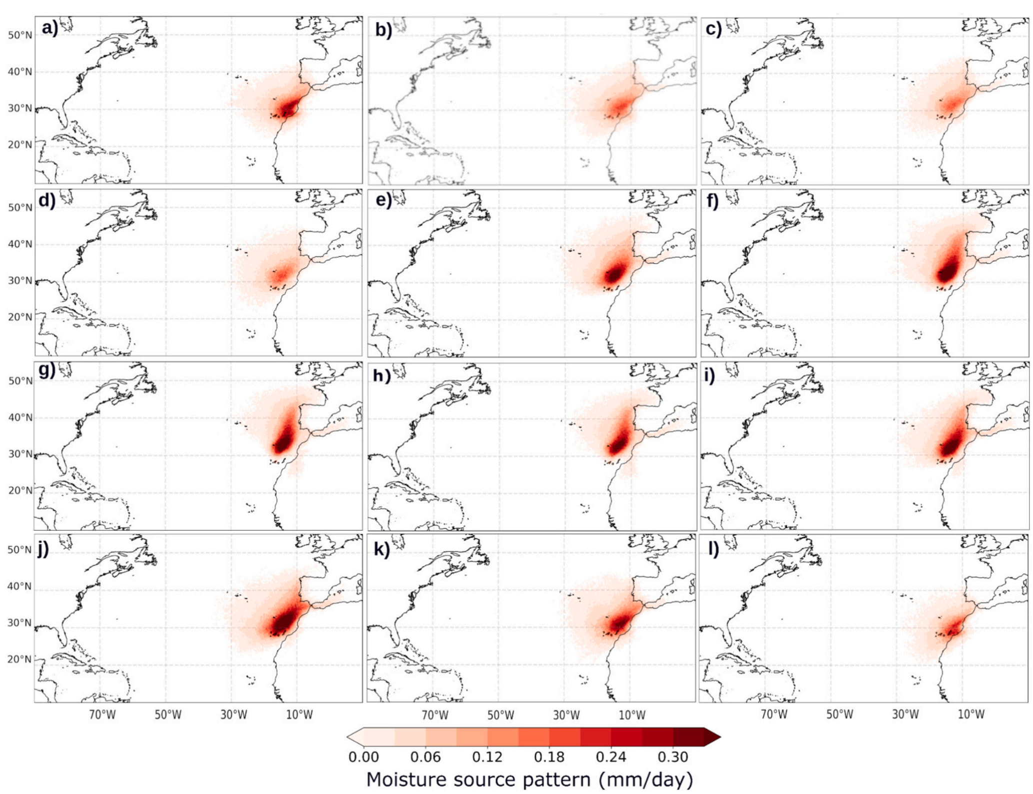

Fig. 4. Monthly moisture source patterns (in mm/day) contributing to the Canary Islands from 1985 to 2022, for the atmospheric layer below 900 hPa. Panels a) to l) correspond to January to December.

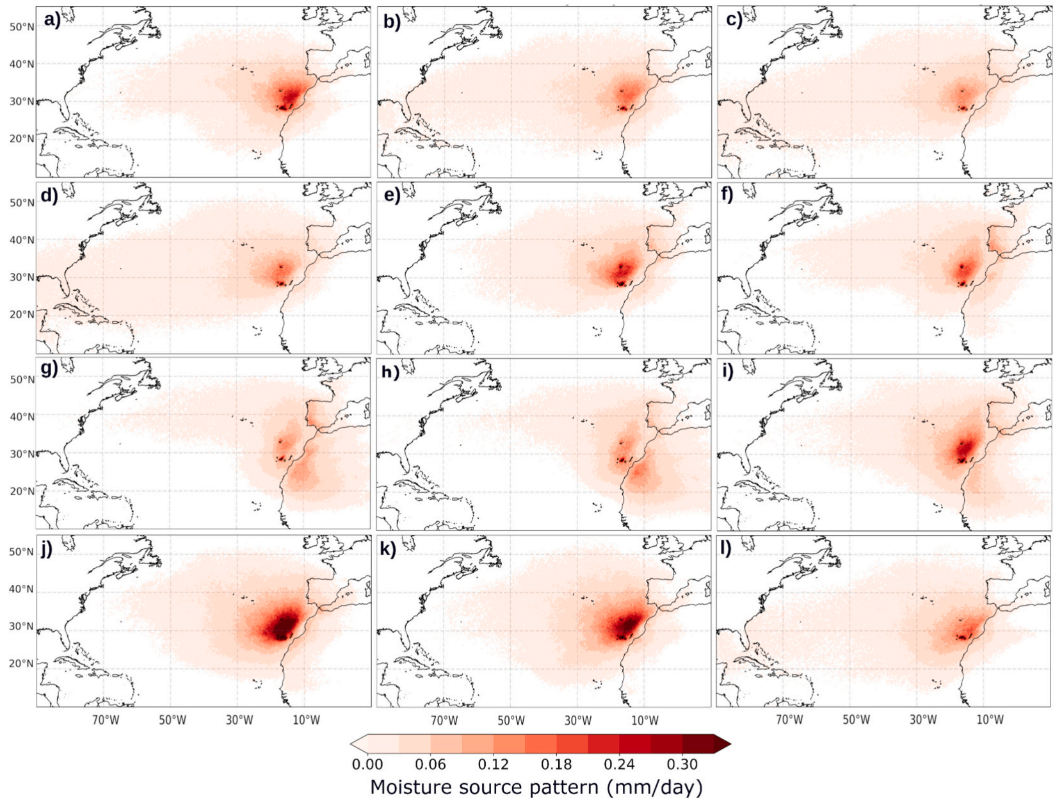

Fig. 5. Monthly moisture source patterns (in mm/day) contributing to the Canary Islands from 1985 to 2022, for the atmospheric layer above 900 hPa. Panels a) to l) correspond to January to December.

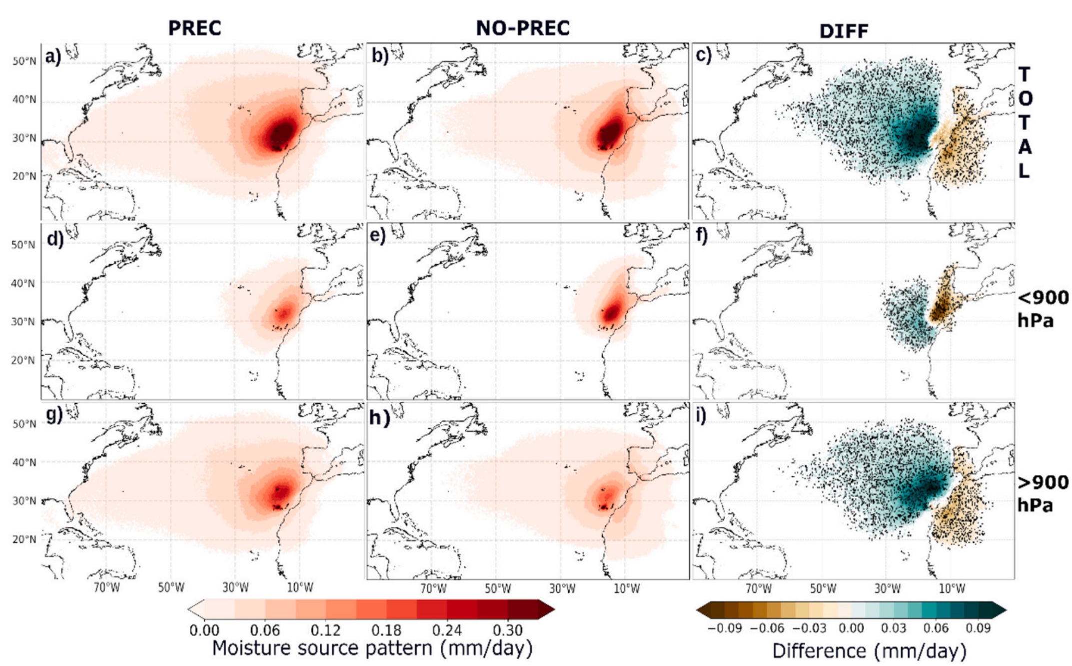

Fig. 6. Moisture source patterns (in mm/day) contributing to the Canary Islands from 1985 to 2022. The first two columns show patterns for days with and without precipitation, and the third shows their differences (day with precipitation minus day without precipitation). The black dots indicate statistically significant anomalies at the 95 % confidence level (based on a Student's *t*-test). Rows represent the fields for the entire atmospheric vertical column, the layer from the surface to 900 hPa, and the layer above 900 hPa.

and 29 % for days without precipitation, respectively (Table S4 of the Supplementary Material). The differences between both patterns (Fig. 6, third column; including a Student *t*-test of significativity at the 95 % level) reveal a greater moisture uptake from the Atlantic Ocean on precipitation days, while for non-precipitation days the contributions predominantly originate from coastal and the northwestern African continent. Again above 900 hPa the percentage contributions (Table S3 of the Supplementary Material) show that for days with precipitation the 59 % of the moisture reaching the Canary Islands comes from the North Atlantic source, while only 4 % comes from Africa and the remainder from southern Europe. However, on days without precipitation, although the North Atlantic remains the main source (with approximately 45 %), an increase of up to 10 % is observed in the contribution from Africa and the remaining percentage from Europe. This result is related to the fact that the relatively drier or even rainless months in the Canary Islands are from April to September (Herrera et al., 2001), which corresponds mainly to the contribution from Africa during the summer months. Furthermore, on these no-precipitation days, the moisture that reaches the archipelago contributes to the formation of a dense layer of low clouds related to the trade winds below the inversion layer (Carrillo et al., 2016).

The differences in the moisture source pattern between days with and without precipitation are also reflected in the differences in the mean sea level pressure (MSLP), geopotential height and IVT fields (Fig. S4 of the Supplementary Material). The MSLP field exhibits negative differences to the north-northeast of the Canary Islands, extending towards central Europe and the Mediterranean Sea, indicating a predominance of low pressures on days with precipitation, which are associated with greater surface instability; in contrast, positive differences stand out over the Atlantic and the African continent. At 500 hPa, instability continues to be present over the region, with negative differences between days with and without precipitation. Finally, IVT differences are positive in the region and over Africa, this reflects the fact that on days with precipitation, water vapour transport is higher in these regions. On days without precipitation, the highest IVT values are observed primarily in the Intertropical Convergence Zone and the eastern North Atlantic.

A monthly analysis of moisture source patterns below and above 900 hPa was also conducted for both precipitation and non-precipitation days. The results (Figs. S5, S6, S7 and S8 of the Supplementary Material) show that in the lower layer, no major differences between both cases are observed and are very similar to the pattern of sources for the overall period. A northward slight shift in the contributions is observed from June to September. The months with the highest moisture contributions for precipitation days are from May to October, whereas for non-precipitation days January and November are also included among the months with higher contributions. In the upper layer, the differences are more pronounced. The moisture source patterns for precipitation days are generally more spatially extensive and exhibit higher contributions. In addition, a notable moisture contribution from the African continent and the Iberian Peninsula is observed from May to November for non-precipitation days, whereas precipitation days are only more pronounced in August and September.

Additionally, the differences in monthly moisture patterns between days with and without precipitation were analyzed for both layers mentioned above (Figs. S9 and S10 of the Supplementary Material). In the layer below 900 hPa, the months with the greatest differences between the two cases were January, October and November, with positive differences in the eastern Atlantic, near the islands and negative differences along the African coast. In the upper layer, positive differences are more prominent over the Atlantic throughout the year, and the most notable negative differences are observed in June, July, October and November.

For precipitation days, the analysis was also done for those days with minimum and maximum precipitation. The 5 % and 95 % quantiles were used as thresholds for the analysis of extreme precipitation, following methodologies employed in previous studies, such as Mondiana et al. (2021), Fan and Chen (2016), and Adeniyi (2016). Furthermore, it is considered that the use of these quantiles would be the most appropriate due to the notable differences in precipitation behaviour among the islands that make up the Canary Islands archipelago. The two sets of data were taken into account as those included in the 5 % (1.2 mm) and 95 % (30.0 mm) quantiles, a total of 1846 and 538 days were recorded, respectively. Fig. 7 displays these moisture source patterns and their anomalies. The moisture source pattern for both quantiles is very similar and the positive anomalies over the central and eastern Atlantic are greater for extreme precipitation in the layer above 900 hPa. Meanwhile, negative anomalies are observed over the African continent and its western coast below 900 hPa for the 95 % quantile. The behaviour of the meteorological variables -MSLP, geopotential height and IVT- supports these findings, revealing differences between the conditions of minimal and maximum precipitation (Figs. S11 and S12 of the Supplementary Material). Conditions of instability are particularly evident at the surface and at 500 hPa for days of extreme precipitation, with increased IVT and greater positive anomalies around the Canary Islands. Furthermore, one of the main factors determining the formation of extreme rainfall in the Canary Islands is the presence of marked instability in the middle layers of the atmosphere (Grimalt et al., 2013; Suárez and Söllheim, 2024). This instability is observed in the geopotential height anomaly field at 500 hPa for days with the 95 % precipitation quantile. These conditions may be related to isolated depressions in the upper levels of the atmosphere known as cut-off lows, with omega-shaped configurations, with deep troughs with different latitudinal positions.

Due to the geographical position of the Canary Islands, previous studies have reported longitudinal differences in precipitation between the western and eastern islands of the Canary archipelago. The western islands (Santa Cruz de Tenerife province) receive significantly more precipitation than the eastern ones (Las Palmas province), hardly exceeding 100 mm/year (Sánchez-Benítez et al., 2017). Furthermore, according to García de Pedraza (1980), the average rainfall in Gran Canaria island (located in the eastern part) is around 120 mm per year (measured at Las Palmas and Gando stations), while in Tenerife island (in the western part) it reaches 550 mm (measured in Los Rodeos and Izaña stations). Considering these local variations, moisture sources were analyzed under three specific conditions: i) days with precipitation in both provinces (Fig. 8, first column), ii) days with precipitation only in Las Palmas province (Fig. 8, second column), and iii) days with precipitation only in Santa Cruz de Tenerife province (Fig. 8, third column). For each of these conditions, 2538, 581 and 1690 days respectively were recorded during the study period. These amounts show that, although the majority of days with precipitation occur in both provinces, Santa Cruz de Tenerife experiences approximately three times more precipitation days than Las Palmas in some seasons, underscoring the stark differences in precipitation patterns across the archipelago.

In general, the moisture source patterns for the three cases are very similar to the pattern observed for precipitation days shown in Fig. 6, with a slight shift to the south in the region with the highest contribution in the case of Santa Cruz de Tenerife. The anomalies for precipitation days in both provinces (Fig. 8, fourth column) are also very consistent with those mentioned in Section 3.2.1. However, notable differences emerge for the other two cases. For precipitation days in the province of Las Palmas, the regions with positive anomalies are predominantly located in the northern sector of the islands (Fig. 8, fifth column), whereas for precipitation days in Santa Cruz de Tenerife, they are located in the west (Fig. 8, sixth column), especially above 900 hPa. These findings highlight the influence of the trade winds on precipitation patterns in the archipelago, especially in summer over Gran Canaria island (Herrera et al., 2001).

The meteorological conditions for the three specific conditions (Figs. S13, S14, and S15 of the Supplementary Material) also reveal differences. The high-pressure patterns in the MSLP fields show a more extended pattern during precipitation days in the province of Las Palmas, and the positive anomalies over the target region stand out. In contrast, for the other two cases, the anticyclone shifts westward, and negative anomalies appear over the Canary Islands, indicating greater atmospheric instability. Regarding the geopotential height fields, negative anomalies are observed across all cases, with more pronounced

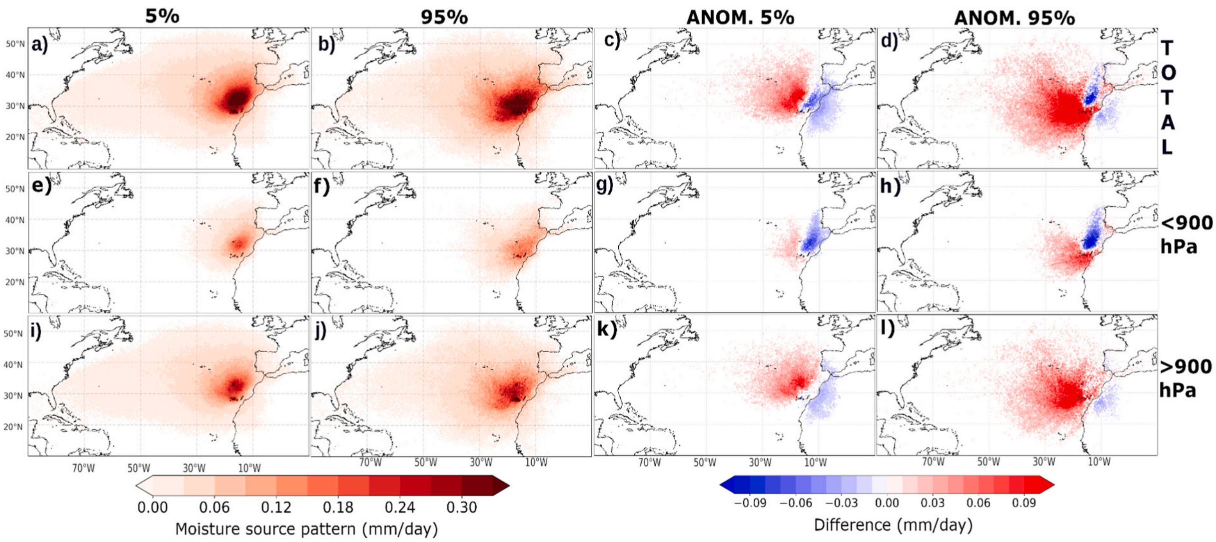

Fig. 7. Moisture source patterns (in mm/day) contributing to the Canary Islands from 1985 to 2022. Columns one and two show moisture sources for the 5 % (extremely dry conditions) and 95 % (extremely wet conditions) precipitation quantiles, while three and four show their anomalies with respect to the historical pattern. Rows represent the fields for the entire atmospheric vertical column, the layer from the surface to 900 hPa, and the layer above 900 hPa.

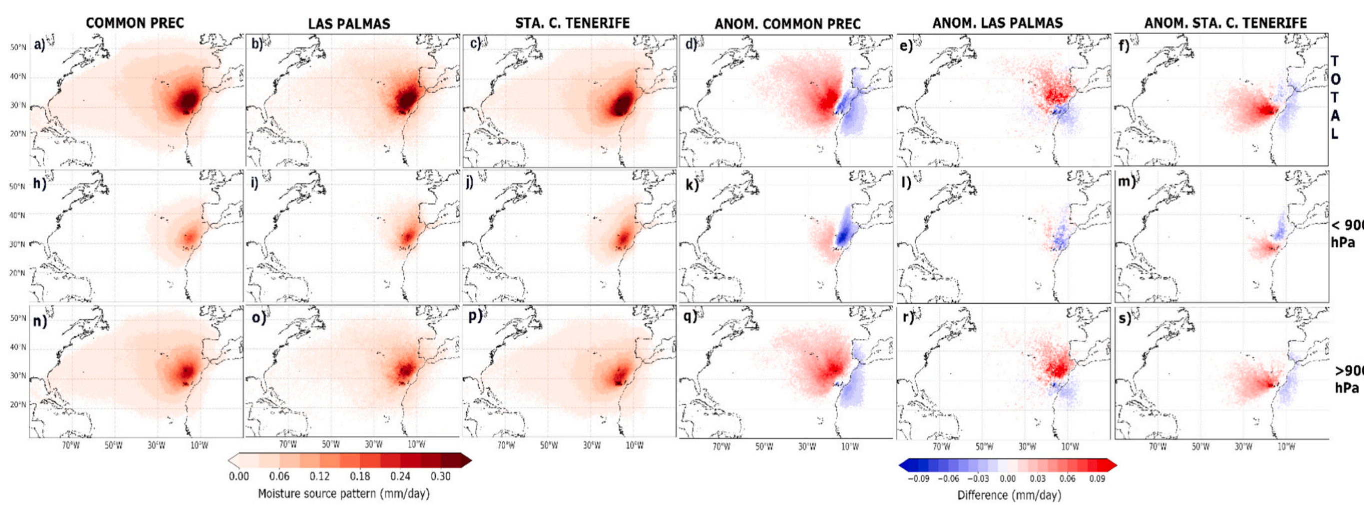

Fig. 8. Moisture source patterns (in mm/day) contributing to the Canary Islands from 1985 to 2022. Columns one to three show moisture sources, and four to six their anomalies with respect to the historical pattern, for days with precipitation in both provinces, only in Las Palmas, and only in Santa Cruz de Tenerife. Rows represent the fields for the entire atmospheric vertical column, the layer from the surface to 900 hPa, and the layer above 900 hPa.

negative anomalies on days with precipitation in both provinces. In the IVT fields, the flow from the Atlantic is evident for the three cases, but with greater intensity over the target region for precipitation days common to both provinces and only in Las Palmas. On days with precipitation in Santa Cruz de Tenerife the flow reaches the Canary Islands from the northwest, while for the other two cases, the flow is from the north. These differences may be related to the moisture source anomalies behaviour. For days with precipitation only in the province of Santa Cruz de Tenerife, the presence of negative anomalies in the target region could indicate that a higher IVT value than the historical pattern is not required. However, for days with precipitation in the province of Las Palmas, and in both provinces, the anomalies are positive, suggesting that, for the occurrence of precipitation in these cases, the IVT presents higher values compared to the historical pattern.

4. Conclusions

This study presents a comprehensive climatological analysis of the moisture sources affecting the Canary Islands from 1985 to 2022, considering seasonal and monthly variations for the entire atmospheric column, with a particular focus on the layers below and above the thermal inversion layer, located near 900 hPa. A dynamic downscaling methodology was applied, using the regional model WRF-ARW, and FLEXPART-WRF forced ERA5 reanalysis data as initial and boundary conditions. It is important to note that the results may be intrinsically influenced by the limitations of the Lagrangian method, as well as by the regionalisation process and the reanalysis datasets used in the study.

Moisture sources were analyzed for different precipitation conditions in the study region using precipitation records from the AEMET. Thise study is novel in that it represents the first climatological assessment of moisture sources in the Canary Islands using a Lagrangian methodology to track the trajectories of potential precipitating particles.

The results indicate that the main moisture sources affecting the Canary Islands come from the North Atlantic throughout most of the year, with approximately 74 % annual contribution. In summer a notable increasing contribution from the African continent occurs, especially above the thermal inversion layer at 900 hPa, reaching up to around 16 %. Below the 900 hPa level, moisture sources tend to be more concentrated, with the highest contribution occurring to the north-northeast, closer to the archipelago. On precipitation days, moisture sources are more intense and extend further into the Atlantic Ocean, with an 81 % contribution from the North Atlantic, compared to non-precipitation days, when the contribution from the North Atlantic decreases to 70 %, and the contribution from northwest Africa rise to 12 %. The anomaly patterns differ in both cases, showing the precipitation days positive anomalies over the Atlantic, whereas non-precipitation days display negative anomalies, a pattern consistent across all months. The atmospheric conditions indicate greater instability and Integrated Vapour Transport (IVT) for precipitation days. The positive anomalies of the moisture source patterns, as well as the anomalies in the analyzed atmospheric conditions, intensified for the most extreme precipitation events.

When precipitation events were analyzed separately for the eastern and western parts of the archipelago, overall larger positive anomalies were observed over the Atlantic in the layer below 900 hPa. However, notable regional differences emerged: on precipitation days, for the eastern islands positive anomalies were predominantly located north of the islands, whereas in the western islands, they appeared westward, mainly in the upper layer (above 900 hPa).

As evident from all the analysis carried out, a key finding of this study is the marked contrast in moisture distribution and contribution to the archipelago above and below 900 hPa, linked to atmospheric stratification and the inversion of the Marine Boundary Layer (MBL). This contrast highlights the critical role of vertical moisture distribution in regional precipitation patterns.

By elucidating the complex interactions between atmospheric moisture sources and precipitation patterns, this study contributes valuable insights for water resource management on the islands, especially in the face of climate change and increasing water scarcity. Furthermore, this knowledge can be used to develop climate change adaptation strategies and plan for extreme weather events. To fill this gap, future studies will further explore the projected changes in moisture sources over the Canary Islands in the future climate, focusing on the middle and end of the century. These studies are crucial to how the future changes may influence precipitation, a region with high water stress, and the associated climatic implications in the Canary Islands. To this end, different climate change scenarios, using CMIP6 model outputs to assess potential shifts in atmospheric dynamics and hydrological processes. We will also analyse possible relationships between future moisture sources and different climate drivers, such as modes of variability like the North Atlantic Oscillation. Improving our understanding of the variability of moisture sources would enrich scientific knowledge and contribute to social resilience by guiding adaptation strategies in water-scarce regions such as the Canary Islands.

CRediT authorship contribution statement

Gleisis Alvarez-Socorro: Writing – review & editing, Writing – original draft, Visualization, Methodology, Investigation, Formal analysis, Data curation, Conceptualization. **José Carlos Fernández-Alvarez:** Writing – review & editing, Methodology, Formal analysis, Data curation, Conceptualization. **Luis Cana:** Writing – review & editing, Supervision, Methodology, Conceptualization. **David Suárez-Molina:** Writing – review & editing, Supervision, Methodology, Data curation, Conceptualization. **Raquel Nieto:** Writing – review & editing, Supervision, Resources, Methodology, Funding acquisition, Conceptualization. **Luis Gimeno:** Writing – review & editing, Supervision, Resources, Methodology, Funding acquisition, Conceptualization.

Funding

This work is supported by the FPU predoctoral contract funded by the Ministerio de Ciencia, Innovación y Universidades, Spain under grant FPU23/02738, by the Xunta de Galicia (Consellería de Cultura, Educación e Universidade) under the Postdoctoral grant IN606B2024/016 and by the SETESTRELO and ESMORGA projects (grant no. PID2021-122314OB-I00 and TED2021-129152B-C43) funded by the Ministerio de Ciencia, Innovación y Universidades, Spain (MCIN/10.13039/501100011033) and Xunta de Galicia (grant ED431C2021/44; Programa de Consolidación e Estructuración de Unidades de Investigación Competitivas (Grupos de Referencia Competitiva), Consellería de Cultura, Educación e Universidade).

Declaration of competing interest

The authors have no relevant financial or non-financial interests that could have appeared to influence the work reported.

Acknowledgements

EPhysLab members are supported by the SETESTRELO and ESMORGA projects (grant no. PID2021-122314OB-I00 and TED2021-129152B-C43) funded by the Ministerio de Ciencia, Innovación y Universidades, Spain (MCIN/10.13039/501100011033) and Xunta de Galicia (grant ED431C2021/44; Programa de Consolidación e Estructuración de Unidades de Investigación Competitivas (Grupos de Referencia Competitiva), Consellería de Cultura, Educación e Universidade). J.C.F.-A. acknowledge FCT for the financial support to CESAM (UIDP/50017/2020, UIDB/50017/2020 & LA/P/0094/2020).

G.A-S acknowledges the financial support from the FPU predoctoral contract funded by the Ministerio de Ciencia, Innovación y Universidades, Spain under grant FPU23/02738. J.C.F.-A. thanks to the support from the Xunta de Galicia (Consellería de Cultura, Educación e Universidade) under the Postdoctoral grant IN606B2024/016.

The authors would especially like to acknowledge AEMET for providing the database for this research. In addition, this work has been possible thanks to the computing resources and technical support provided by CESGA (Centro de Supercomputación de Galicia) and Red Española de Supercomputación (RES) (AECT-2022-3-0009 and DATA-2021-1-0005). We are grateful to the agreement between the University of Vigo and Elsevier for Open Access publication.

Appendix A. Supplementary data

Supplementary data to this article can be found online at https://doi.org/10.1016/j.atmosres.2025.108312.

Data availability

The precipitation data were obtained from AEMET's National Climate Data Bank and it has been recorded by AEMET's in-situ observation network across the Canary Islands. The data used can be downloaded online for free. The ERA5 reanalysis (Hersbach et al., 2020) and outputs of the CESM2 climate model (Danabasoglu et al., 2020) were used as forces for the WRF-ARW regional climate model. The technical and physical details of the WRF-ARW model are presented by Skamarock et al. (2008) and the dispersion model FLEXPART-WRF by Brioude et al. (2013). The TROVAv1.0 software (Fernández-Alvarez et al., 2022) was downloaded from https://github.com/tramo-ephyslab/TROVA-master/.

References

Adeniyi, M.O., 2016. The consequences of the IPCC AR5 RCPs 4.5 and 8.5 climate change scenarios on precipitation in West Africa. Clim. Chang. 139, 245–263. https://doi.org/10.1007/s10584-016-1774-2.

AEMET, 2012. Climate Atlas of the Archipelagos of the Canary Islands, Madeira and the Azores. The Meteorological State Agency of Spain and the Institute of Meteorology, Portugal. https://doi.org/10.1016/j.cliser.2024.100487.

Arnault, J., Jung, G., Haese, B., Fersch, B., Rummler, T., Wei, J., Zhang, Z., Kunstmann, H., 2021. A Joint Soil-Vegetation-Atmospheric Modeling Procedure of Water Isotopologues: Implementation and Application to different climate zones

with WRF-Hydro-Iso. J. Adv. Model. Earth Syst. 13. https://doi.org/10.1029/2021MS002562.
Bechtel, B., 2016. The Climate of the Canary Islands by Annual Cycle Parameters. https://doi.org/10.5194/isprsarchives-XLI-B8-243-2016.
Bershaw, J., 2018. Controls on deuterium excess across Asia. Geosci 8 (7), 257. https://doi.org/10.3390/geosciences8070257.
Brioude, J., Arnold, D., Stohl, A., Cassiani, M., Morton, D., et al., 2013. The Lagrangian particle dispersion model FLEXPART-WRF version 3.1. Geosci. Model Dev. 6 (6), 1889–1904. https://doi.org/10.5194/gmd-6-1889-2013.
Carrillo, J., Guerra, J.C., Cuevas, E., Barrancos, J., 2016. Characterization of the marine boundary layer and the trade-wind inversion over the sub-tropical North Atlantic. Boundary-Layer Meteorol. 158, 311–330. https://doi.org/10.1007/s10546-015-0081-1.
Cheng, T.F., Lu, M., 2023. Global lagrangian tracking of continental precipitation recycling, footprints, and cascades. J. Clim. 36, 1923–1941. https://doi.org/10.1175/JCLI-D-22-0185.1.
Coll-Hidalgo, P., Nieto, R., Fernández-Álvarez, J.C., Gimeno, L., 2025. Assessment of the origin of moisture for the precipitation of North Atlantic extratropical cyclones: insights from downscaled ERA5. Atmos. Res. 324. https://doi.org/10.1016/j.atmosres.2025.108205.
Cropper, T.E., Hanna, E., 2014. An analysis of the climate of Macaronesia, 1865-2012. Int. J. Climatol. 34 (3), 604–622. https://doi.org/10.1002/joc.3710.
Dahinden, F., Aemisegger, F., Wernli, H., Schneider, M., et al., 2021. Disentangling different moisture transport pathways over the eastern subtropical North Atlantic using multi-platform isotope observations and high-resolution numerical modelling. Atmos. Chem. Phys. 21 (21), 16319–16347. https://doi.org/10.5194/acp-21-16319-2021.
Dahinden, F., Aemisegger, F., Wernli, H., Pfahl, S., 2023. Unravelling the transport of moisture into the Saharan Air Layer using passive tracers and isotopes. Atmos. Sci. Lett. 24. https://doi.org/10.1002/asl.1187.
Danabasoglu, G., Lamarque, J.F., Bacmeister, J., Bailey, D.A., DuVivier, A.K., Edwards, J., et al., 2020. The community earth system model version 2 (CESM2). J. Adv. Model. Earth Syst. 12 (2), e2019MS001916. https://doi.org/10.1029/2019MS001916.
Eiras-Barca, J., Fernández-Álvarez, J.C., Alvarez-Socorro, G., Rahimi-Esfarjani, S., Carrasco-Pena, P., Nieto, R., Gimeno, L., 2025. Projected changes in moisture sources and sinks affecting the US East Coast and the Caribbean Sea. Ann. N. Y. Acad. Sci. https://doi.org/10.1111/nyas.15289.
Fan, L., Chen, D., 2016. Trends in extreme precipitation indices across China detected using quantile regression. Atmos. Sci. Lett. 17 (7), 400–406. https://doi.org/10.1002/asl.671.
Fernández-Alvarez, J.C., 2023. Future Changes in Atmospheric Moisture and Wind Field Using Numerical Simulations: Implications for Moisture Transport and Wind Energy. Doctoral Dissertation. University of Vigo, Spain. http://hdl.handle.net/11093/6340.
Fernández-Alvarez, J.C., Pérez-Alarcón, A., Nieto, R., Gimeno, L., 2022. TROVA: TRansport of water VApor. SoftwareX 20, 101228. https://doi.org/10.1016/j.softx.2022.101228.
Fernández-Alvarez, J.C, Alvarez-Socorro, G., Durán-Quesada, AM., Nieto, R., Gimeno, L., 2025. Future Changes in the Contribution of Gulf of Mexico-Caribbean Sea Moisture Source: Impacts on Regional Precipitation Patterns. Earth Syst. Environ. 9, 1083–1097. https://doi.org/10.1007/s41748-024-00532-8.
Fernández-Alvarez, J.C., Pérez-Alarcón, A., Eiras-Barca, J., Rahimi, S., Nieto, R., Gimeno, L., 2023b. Projected changes in atmospheric moisture transport contributions associated with climate warming in the North Atlantic. Nat. Commun. 14 (1), 6476. https://doi.org/10.1038/s41467-023-41915-1.
Fernández-Alvarez, J.C., Vázquez, M., Pérez-Alarcón, A., Nieto, R., Gimeno, L., 2023c. Comparison of moisture sources and sinks estimated with different versions of FLEXPART and FLEXPART-WRF models forced with ECMWF reanalysis data. J. Hydrometeorol. 24 (2), 221–239. https://doi.org/10.1175/JHM-D-22-0018.1.
Francisco-Ortega, J., Santos-Guerra, A., Bacallado, J.J., Gillespie, R.G., Clague, D.A., 2009. Canary islands, biology. In: Encyclopedia of Islands. University of California Press, Berkeley, pp. 127–133. https://doi.org/10.1525/9780520943728-031.
Fremme, A., Sodemann, H., 2019. The role of land and ocean evaporation on the variability of precipitation in the Yangtze River valley. Hydrol. Earth Syst. Sci. 23, 2525–2540. https://doi.org/10.5194/hess-23-2525-2019.
García de Pedraza, L., 1980. Aspectos meteorológicos de las Islas Canarias. Repositorio AEMET 156–173. https://repositorio.aemet.es/handle/20.500.11765/684.
García-Herrera, R., Gallego, D., Hernández, E., Gimeno, L., Ribera, P., Calvo, N., 2003. Precipitation trends in the Canary Islands. Int. J. Climatol. 23, 235–241. https://hdl.handle.net/20.500.14352/51083.
Gimeno, L., Vázquez, M., Eiras-Barca, J., Sorí, R., Stojanovic, M., Algarra, I., Nieto, R., Ramos, A.M., Durán-Quesada, A.M., Dominguez, F., 2020. Recent progress on the sources of continental precipitation as revealed by moisture transport analysis. Earth Sci. Rev. 201 (103), 070. https://doi.org/10.1016/j.earscirev.2019.103070.
Gimeno, L., Eiras-Barca, J., Durán-Quesada, A.M., et al., 2021. The residence time of water vapour in the atmosphere. Nat. Rev. Earth Environ. 2 (8), 558–569. https://doi.org/10.1038/s43017-021-00181-9.
Grimalt, M., Tomàs, M., Alomar, G., Martin-Vide, J., Moreno-García, M.D.C., 2013. Determination of the Jenkinson and Collison's weather types for the western Mediterranean basin over the 1948-2009 period. Temporal analysis. Atmósfera 26 (1), 75–94.
Grindinger, C.M., 1992. Temporal variability of the trade wind inversion: Measured with a boundary layer vertical profiler (Order No. 28642009). ProQuest Dissertations & Theses Global. Available from (2540756967). https://www.proquest.com/dissertations-theses/temporal-variability-trade-wind-inversion/docview/2540756967/se-2.
Guerra, J.C., Rodrıguez, S., Arencibia, M.T., Garcıa, M.D., 2004. Study on the formation and transport of ozone in relation to the air quality management and vegetation protection in Tenerife (Canary Islands). Chemosphere 56 (11), 1157–1167. https://doi.org/10.1016/j.chemosphere.2004.03.017.
Guerra, J.C., Regalado, C.M., Ritter, A., León-González, M., 2023. Stable isotopic composition of fog and rainfall in a Macaronesian cloud forest. J. Hydrometeorol. 622, 129763. https://doi.org/10.1016/j.jhydrol.2023.129763.
Herrera, R.G., Puyol, D.G., Martín, E.H., Presa, L.G., Rodríguez, P.R., 2001. Influence of the North Atlantic oscillation on the Canary Islands precipitation. J. Clim. 14 (19), 3889–3903. https://doi.org/10.1175/1520-0442(2001)014<3889:IOTNAO>2.0.CO;2.
Hersbach, H., Bell, B., Berrisford, P., Hirahara, S., Horányi, A., Muñoz-Sabater, J., et al., 2020. The ERA5 global reanalysis. Q. J. R. Meteorol. Soc. 146 (730), 1999–2049. https://doi.org/10.1002/qj.3803.
Holgate, C.M., Evans, J.P., van Dijk, A.I.J.M., Pitman, A.J., Di Virgilio, G., 2020. Australian precipitation recycling and evaporative source regions. J. Clim. 33, 8721–8735. https://doi.org/10.1175/JCLI-D-19-0926.1.
Insua-Costa, D., Miguez-Macho, G., 2018. A new moisture tagging capability in the Weather Research and forecasting model: Formulation, validation and application to the 2014 Great Lake-effect snowstorm. Earth Syst. Dynam. 9, 167–185. https://doi.org/10.5194/esd-9-167-2018.
Insua-Costa, D., Miguez-Macho, G., Llasat, M.C., 2019. Local and remote moisture sources for extreme precipitation: a study of the two catastrophic 1982 western Mediterranean episodes. Nat. Hazards Earth Syst. Sci. 23, 3885–3900. https://doi.org/10.5194/hess-23-3885-2019.
Izquierdo, R., Belmonte, J., Avila, A., Alarcón, M., Cuevas, E., Alonso-Pérez, S., 2011. Source areas and long-range transport of pollen from continental land to Tenerife (Canary Islands). Int. J. Biometeorol. 55, 67–85. https://doi.org/10.1007/s00484-010-0309-1.
Keune, J., Schumacher, D.L., Miralles, D.G., 2022. A unified framework to estimate the origins of atmospheric moisture and heat using Lagrangian models. Geosci. Model Dev. 15, 1875–1898. https://doi.org/10.5194/gmd-15-1875-2022.
Läderach, A., Sodemann, H., 2016. A revised picture of the atmospheric moisture residence time. Geophys. Res. Lett. 43 (2), 924–933. https://doi.org/10.1002/2015GL067449.
Li, J., Zhao, Y., Chen, D., Zhao, P., Zhang, C., Wang, Y., 2024. The quantitative role of moisture and vertical motion in shaping summer heavy rainfall over North China under two distinct large-scale weather patterns. J. Clim. 37 (8), 2655–2672. https://doi.org/10.1175/JCLI-D-22-0850.1.
Martín, J.L., Bethencourt, J., Cuevas-Agulló, E., 2012. Assessment of global warming on the island of Tenerife, Canary Islands (Spain). Trends in minimum, maximum and mean temperatures since 1944. Clim. Chang. https://doi.org/10.1007/s10584-012-0407-7.
Mestre-Barceló, A., Chazarra-Bernabé, A., Pires, V., Cunha, S., Silva, A., Marques, J., Carvalho, F., Mendes, M., Neto, J., 2012. Climate atlas of the Archipelagos of the Canary Islands, Madeira and Azores. Air temperature and precipitation (1971–2000). Agencia Estatal de Meteorología and Instituto de Meteorologia de Portugal (eds), p. 80. https://www.aemet.es/documentos/es/conocermas/recursos_en_linea/publicaciones_y_estudios/publicaciones/2Atlas_climatologico/Atlas_Clima_Macaronesia__Baja.pdf.
Mondiana, Y.Q., Zairina, A., Sari, R.K., 2021. Quantile regression modeling to predict extreme precipitation. J. Phys. Conf. Ser. 1918 (4), 042031. IOP Publishing. https://doi.org/10.1088/1742-6596/1918/4/04203.
Numaguti, A., 1999. Origin and recycling processes of precipitating water over the Eurasian continent: experiments using an atmospheric general circulation model. J. Geophys. Res. 104, 1957–1972. https://doi.org/10.1029/1998JD200026.
Pérez, J.C., Díaz, J.P., González, A., Expósito, J., Rivera López, F., Taima, D., 2014. Evaluation of WRF parameterizations for dynamical downscaling in the Canary Islands. J. Clim. 27, 5611–5631. https://doi.org/10.1175/JCLI-D-13-00458.1.
Polade, S.D., Pierce, D.W., Cayan, D.R., Gershunov, A., Dettinger, M.D., 2014. The key role of dry days in changing regional climate and precipitation regimes. Sci. Rep. 4, 4364. https://doi.org/10.1038/srep04364.
Ramos, A.M., Trigo, R.M., Tomé, R., Liberato, M.L., 2018. Impacts of atmospheric rivers in extreme precipitation on the European Macaronesian Islands. Atmosphere 9 (8), 325. https://doi.org/10.3390/atmos9080325.
Rodríguez, S., Torres, C., Guerra, J.C., Cuevas, E., 2004. Transport pathways of ozone to marine and free-troposphere sites in Tenerife, Canary Islands. Atmos. Environ. 38 (28), 4733–4747. https://doi.org/10.1016/j.atmosenv.2004.05.021.
Rodríguez, S., Alastuey, A., Alonso-Pérez, S., Querol, X., Cuevas, E., Abreu-Afonso, J., Viana, M., Pérez, N., Pandolfi, M., de la Rosa, J., 2011. Transport of desert dust mixed with North African industrial pollutants in the subtropical Saharan Air Layer. Atmos. Chem. Phys. 11 (13), 6663–6685. https://doi.org/10.5194/acp-11-6663-2011.
Romero Campos, P.M., de la Marrero Santa Cruz, C.L., Alonso Pérez, S., Cuevas Agulló, E., Afonso Gómez, S., Ortiz de Galisteo, J.P., 2011. Una climatología del agua precipitable en la región subtropical sobre la isla de Tenerife basada en datos de radiosondeos. In: Nota Técnica 6 de AEMET. https://doi.org/10.31978/281-12-007-5.
Sánchez-Benítez, A., García-Herrera, R., Vicente-Serrano, S.M., 2017. Revisiting precipitation variability, trends and drivers in the Canary Islands. Int. J. Climatol. 37 (9), 3565–3576. https://doi.org/10.1002/joc.4937.
Sancho, P., De La Cruz, J., Díaz, A., Martín, F., Hernández, E., Valero, F., Albarran, B., 1992. A five-year climatology of back-trajectories from the Izaña baseline station, Tenerife, Canary Islands. Atmos. Environ. Part A Gen. Top. 26 (6), 1081–1096. https://doi.org/10.1016/0960-1686(92)90040-R.

Sanz, R., David Suárez-Molina, D., Díaz, B., Marrero, R., 2022. Ondas tropicales en Canarias. Calend. Meteorol. 2018-2022, 266–272. http://hdl.handle.net/20.500.11765/13568.

Schär, C., Ban, N., Fischer, E.M., Rajczak, J., Schmidli, J., Frei, C., et al., 2016. Percentile indices for assessing changes in heavy precipitation events. Clim. Chang. 137, 201–216. https://doi.org/10.1007/s10584-016-1669-2.

Skamarock, W.C., Klemp, J.B., Dudhia, J., Gill, D.O., Barker, D.M., Duda, M.G., et al., 2008. A description of the advanced research WRF version 3. NCAR Tech. Note 475 (125), 10–5065. https://opensky.ucar.edu/islandora/object/technotes%3A500/datastream/PDF/download/A_Description_of_the_Advanced_Research_WRF_Version_3.citation.

Sodemann, H., Schwierz, C., Wernli, H., 2008. Interannual variability of Greenland winter precipitation sources: Lagrangian moisture diagnostic and North Atlantic Oscillation influence. J. Geophys. Res. Atmos. 113 (D03), 107. https://doi.org/10.1029/2007jd008503.

Stohl, A., James, P.A., 2004. Lagrangian analysis of the atmospheric branch of the global water cycle. Part I: Method description, validation, and demonstration for the August 2002 flooding in Central Europe. J. Hydrometeorol. 5, 656–678. https://doi.org/10.1175/1525-7541(2004)005<0656:ALAOTA>2.0.CO;2.

Suárez, P.M., Söllheim, Á.L., 2024. Identification of the Synoptic Causes of Torrential Rainfall events in the Canary Islands (1950–2020). Atmosphere 15 (12), 1537. https://doi.org/10.3390/atmos15121537.

Tuinenburg, O.A., Staal, A., 2020. Tracking the global flows of atmospheric moisture and associated uncertainties. Hydrol. Earth Syst. Sci. 24, 2419–2435. https://doi.org/10.5194/hess-24-2419-2020.

Van Der Ent, R.J., Tuinenburg, O.A., 2017. The residence time of water in the atmosphere revisited. Hydrol. Earth Syst. Sci. 21, 779–790. https://doi.org/10.5194/hess-21-779-2017.

Van der Ent, R., Wang-Erlandsson, L., Keys, P.W., Savenije, H., 2014. Contrasting roles of interception and transpiration in the hydrological cycle–part 2: Moisture recycling. Earth Syst. Dynam. 5, 471–489. https://doi.org/10.5194/esd-5-471-2014.

Viana, M., Querol, X., Alastuey, A., Cuevas, E., Rodrıguez, S., 2002. Influence of African dust on the levels of atmospheric particulates in the Canary Islands air quality network. Atmos. Environ. 36 (38), 5861–5875. https://doi.org/10.1016/S1352-2310(02)00463-6.

Zhao, Y., Li, J., Tian, Y., Li, J., 2024. Distinguishing extreme precipitation mechanisms associated with atmospheric rivers and nonatmospheric rivers in the lower Yangtze river basin. J. Clim. 37 (15), 3995–4010. https://doi.org/10.1175/JCLI-D-23-0400.1.

Zhou, K., Shi, X., 2024. Understanding precipitation moisture sources and their dominant factors during droughts in the Vietnamese Mekong Delta. Water Resour. Res. 60 (7), e2023WR035920. https://doi.org/10.1029/2023WR035920.